Correlation energy of the uniform electron gas from an interpolation between high- and low-density limits

Jianwei Sun and John P. Perdew
Department of Physics and Quantum Theory Group, Tulane University, New Orleans, Louisiana 70118, USA

Michael Seidl
Institute of Theoretical Physics, University of Regensburg, 93040 Regensburg, Germany

(Received 22 October 2009; revised manuscript received 4 February 2010; published 24 February 2010)

We show that known or knowable information about the high-($r_s \to 0$) and low-density ($r_s \to \infty$) asymptotes can be used to predict the correlation energy per electron, $e_c(r_s,\zeta)$, of the three-dimensional uniform gas over the whole range of the density parameter ($0 \le r_s < \infty$) and relative spin polarization ($0 \le |\zeta| \le 1$), without quantum Monte Carlo or other input. For $\zeta=0$, the high-density limit through order r_s is known exactly from many-body perturbation theory, and for all ζ, the low-density limit through order $1/r_s^2$ is known accurately from a simple, intuitive, and accurate model. We propose a single interpolation formula with the expected analytic structure to all orders in both limits, and use it to predict $e_c(r_s,0)$ in excellent agreement with quantum Monte Carlo data. For $|\zeta|>0$, we derive the ζ dependence of the coefficient $a_1(\zeta)$ of the $r_s \ln r_s$ term, previously known only for $|\zeta|=0$ and 1. For $b_1(\zeta)$, the coefficient of the r_s term (not yet derived for $\zeta \neq 0$), we approximately extend the known $b_1(0)$ by using a simplification of the available quantum Monte Carlo information that replaces the second-order transition over $50 < r_s < 100$ by a sudden transition to full spin polarization at $r_s=75$.

DOI: 10.1103/PhysRevB.81.085123 PACS number(s): 71.10.Ca, 71.15.Mb, 31.15.E−

I. INTRODUCTION

The uniform electron gas[1] has long been a paradigm for condensed-matter physics. In the 1930s, Wigner[2] proposed a rough interpolation ($-\alpha/[r_s+\beta]$) of its correlation energy per electron e_c, as a function of the density parameter or average neighbor distance (r_s) in bohr, between approximate high-density (or weakly interacting) and low-density (or strongly interacting) limits, and so was able to explain the cohesion of the alkali metals. Because the uniform gas has no energy gap, its correlation energy diverges in lowest order ε^4 (where $-\varepsilon$ is the charge on the electron) or r_s^0. In the 1950s, many-body approaches including the random-phase approximation (RPA) (Refs. 3 and 4) produced a finite e_c by summing subsets of perturbation-theory terms to all orders. Gell-Mann and Brueckner[5] showed that many-body theory could predict exactly the leading terms ($a_0 \ln r_s + b_0$) of the high-density expansion, where a_0 comes from RPA alone and b_0 includes also second-order exchange. Approximate many-body theories also predicted $e_c(r_s)$ over the range of physical densities, and some of these[6,7] were confirmed[8,9] by the diffusion quantum Monte Carlo (QMC) calculations of the 1980s and later.[10–15]

The uniform electron gas assumed a new importance in the 1960s and later, when the density-functional theory of Kohn and Sham[16] showed how to use an analytic parametrization of $e_c(r_s,\zeta)$, where ζ is the relative spin polarization, to make useful but approximate calculations for real atoms, molecules, and solids. It is not only the local spin-density approximation but also most higher-level approximations,[17] that need such a parametrization. There are three widely used parametrizations [Perdew-Zunger (PZ),[18] Vosko-Wilk-Nusair (VWN),[19] and Perdew-Wang (PW92) (Ref. 20)], all based on the same QMC (Ref. 10) and all in close agreement[21] over the valence-electron range $1 < r_s < 10$. These parametrizations are constrained to respect the leading order of the high-density expansion but are still highly fitted to QMC. For example, VWN and PW92 each have nine fit parameters. There are also at least two other parametrizations based on correlation-hole models.[22,23]

Further work has refined the expansion coefficients of the leading order of the high-density limit[24] or extended them to the fully or partly spin-polarized case,[18,19,25,26] or derived coefficients in the next order.[20,27–29] It is now possible to see if a sophisticated generalization of the Wigner interpolation can use this information to predict e_c for all r_s and ζ. This possibility was proposed in Ref. 20, before all the needed ingredients were available. As we will see, such an interpolation between the high- and low-density limits ("density-parameter interpolation" or DPI) can be accurate, even without QMC or other input. It confirms the adequacy of the widely used parametrizations and their underlying QMC calculations while definitely improving them in the extreme limits $r_s \ll 1$ and $r_s \gg 50$. Interpolations of a similar kind ["interaction strength interpolations" or ISI (Refs. 30 and 31)] have also proven useful for inhomogeneous electronic systems.[30–33] While the QMC calculations for the uniform-gas suffice for practical purposes, these calculations are numerically challenging (relaxation of the fixed node approximation, extrapolation from finite supercells, practical limitations on the number of r_s and ζ values included, etc.), leading to some discrepancies among different QMC calculations.[10–15] In the more difficult case of the jellium surface energy,[8,34] the earlier QMC calculations[35] were much less accurate than standard density functional[8,34] or later QMC (Refs. 36 and 37) calculations.

The three-dimensional (3D) uniform electron density ρ is fixed by the dimensionless density parameter (Seitz radius) r_s,

TABLE I. The coefficients (in hartree) of the high-density ($r_s \to 0$) and low-density ($r_s \to \infty$) expansions for the uniform-gas correlation energy in the Perdew-Zunger (PZ) (Ref. 18), Vosko-Wilk-Nusair (VWN) (Ref. 19), Perdew-Wang (PW92) (Ref. 20), and present DPI expressions, for the spin-unpolarized ($\zeta=0$) and fully polarized ($\zeta=1$) cases. Asterisks denote coefficients constrained to exact or near-exact values. The other coefficients are from analytic fits to the quantum Monte Carlo results of Ref. 10. The low-density coefficients f_0, f_1, and f_2 in the present DPI expression are calculated within the accurate PC model (Refs. 30 and 41) while those in parentheses are from the Wigner-crystal calculation of Ref. 42. The coefficients $c_x(\zeta)$ and $c_s(\zeta)$ at $\zeta=0,1$ are $c_x(0)=-0.458165$, $c_x(1)=-0.577252$, $c_s(0)=1.104951$, and $c_s(1)=1.754000$, respectively.

	PZ	VWN	PW92	DPI
$a_0(0)$	0.0311*	0.03109*	0.03109*	0.03109*
$b_0(0)$	−0.048*	−0.04665*	−0.04664*	−0.04692*
$a_1(0)$	0.0020	0.0	0.00664	0.009229*
$b_1(0)$	−0.0116	−0.08775	−0.01043	−0.010*
$f_0(0)$	−0.8850	−1.03543	−0.8917	−0.9*(−0.896)
$f_1(0)$	1.3479	1.03045	1.4408	1.5*(1.33)
$f_2(0)$	−1.8717	0.9039	−2.5565	0.0*(−0.37)
$a_0(1)$	0.01555*	0.01555*	0.01555*	0.01554*
$b_0(1)$	−0.0269*	−0.02555*	−0.02560*	−0.02574*
$a_1(1)$	0.0007	0.0	0.00319	0.003125*
$b_1(1)$	−0.0048	−0.01956	−0.00384	−0.006749
$f_0(1)$	−0.9001	−1.2736	−0.9060	−0.9*
$f_1(1)$	1.7288	1.4969	1.7697	1.5*
$f_2(1)$	−6.2667	−3.3180	−6.1163	0.0*

$$\rho = \left[\frac{4\pi}{3}(r_s a_B)^3\right]^{-1} = \rho_\uparrow + \rho_\downarrow \tag{1}$$

with the densities $\rho_\uparrow$ and $\rho_\downarrow$ of up- and down-spin electrons, respectively. Here, $a_B=\hbar^2/(me^2)$ is the Bohr radius. The spin polarization ζ is given by

$$\zeta \equiv \frac{\rho_\uparrow - \rho_\downarrow}{\rho} \Leftrightarrow \rho_{\uparrow,\downarrow} = \rho\frac{1 \pm \zeta}{2}. \tag{2}$$

Accounting for a neutralizing positive background, the total energy per particle is

$$e_{\rm tot}(r_s,\zeta) = t_s(r_s,\zeta) + e_x(r_s,\zeta) + e_c(r_s,\zeta). \tag{3}$$

The first two terms on the right-hand side are, respectively, the noninteracting kinetic and exchange energies,

$$t_s(r_s,\zeta) = \frac{c_s(\zeta)}{r_s^2}, \quad e_x(r_s,\zeta) = \frac{c_x(\zeta)}{r_s}. \tag{4}$$

(We are using atomic units where $\hbar=m=e^2=1$.) The exact coefficients $c_s(\zeta)$ and $c_x(\zeta)$ are given in Tables I and II. Correlation suppresses fluctuations of the electron density.[38] The correlation energy appears to have the small-r_s (high-density) asymptotic expansion,[3,27,28,39]

TABLE II. The coefficients (in hartree), as functions of the relative spin polarization ζ, in the high-density ($r_s \to 0$) expansions for the energy of the 3D uniform electron gas. $c_s(\zeta)$ and $c_x(\zeta)$ are exact (Ref. 20). Explicit exact expressions for $a_0(\zeta)$ and $b_0(\zeta)$ are available but rather complicated; see Eq. (32) of Ref. 26 and Eq. (20) of Ref. 25. $a_1(\zeta)$ has only the integral expression given in Appendix A. All these coefficients of the high-density limit are represented here by accurate fits (see Fig. 2). The exact $a_1(\zeta)$ has infinite slope at $|\zeta|=1$ (see Fig. 2(c)), and the corresponding basis functions $\arcsin(\zeta^{2n})$, with $n=1$ to 4, have been chosen to recover this feature. The coefficients in this table are used consistently throughout this work.

$c_s(\zeta)$	$\frac{3}{10}(\frac{9\pi}{4})^{2/3}\frac{1}{2}[(1+\zeta)^{5/3}+(1-\zeta)^{5/3}]$
$c_x(\zeta)$	$-\frac{3}{4\pi}(\frac{9\pi}{4})^{1/3}\frac{1}{2}[(1+\zeta)^{4/3}+(1-\zeta)^{4/3}]$
$a_0(\zeta)$	$[-35.57\zeta^8+50.44\zeta^6-24.76\zeta^4-5.66\zeta^2+31.09]\times 10^{-3}$
$b_0(\zeta)$	$[-21.36\zeta^8+36.43\zeta^6-13.58\zeta^4+19.69\zeta^2-46.92]\times 10^{-3}$
$a_1(\zeta)$	$[9.229+0.2263\ \arcsin(\zeta^2)-17.61\ \arcsin(\zeta^4)$ $+36.70\ \arcsin(\zeta^6)-23.20\ \arcsin(\zeta^8)]\times 10^{-3}$

$$e_c(r_s,\zeta) = \sum_{n=0}^{\infty}[a_n(\zeta)\ln(r_s) + b_n(\zeta)]r_s^n \quad (r_s \to 0). \tag{5}$$

The coefficients $a_0(\zeta)$, $a_1(\zeta)$, and $b_0(\zeta)$, which arise from RPA (ring diagrams) and from second-order exchange, are known or evaluated here exactly (Appendix A). The coefficient $b_1(\zeta)$, which can have a more complicated many-body origin (including ladder diagrams and higher-order exchange), has been evaluated only for $\zeta=0$.[28]

In the opposite low-density limit $r_s \to \infty$ for the uniform fluid phase, where the electronic behavior is similar[30] to zero-point oscillations of the electrons about equilibrium positions in a Wigner crystal, we expect the total energy [Eq. (3)] to become strictly independent of ζ,[20]

$$e_{\rm tot}(r_s,\zeta) = f_0/r_s + f_1/r_s^{3/2} + f_2/r_s^2 + \cdots.$$

Therefore,

$$e_c(r_s,\zeta) = \frac{f_0 - c_x(\zeta)}{r_s} + \frac{f_1}{r_s^{3/2}} + \frac{f_2 - c_s(\zeta)}{r_s^2} + \sum_{n=3}^{\infty}\frac{f_n}{r_s^{1+n/2}} + e_{\rm exp}(r_s,\zeta) \quad (r_s \to \infty) \tag{6}$$

with constant (ζ independent) coefficients f_n. The contribution $e_{\rm exp}(r_s,\zeta) \sim \exp[-g(\zeta)r_s^{1/2}]$ arises[40] from the exponential overlap of localized one-electron states. Since the density parameter r_s is dimensionless, the coefficients in Eqs. (4)–(6) all have units of hartree.

Figure 1 shows the idea behind and the result of our interpolation. Note that the high-density limit is reasonably accurate for $r_s<1$, and the low-density limit for $r_s>50$. The ratio $e_c(r_s,1)/e_c(r_s,0)$ grows slowly from 0.5 to 0.73 as r_s grows from 0 to ∞.

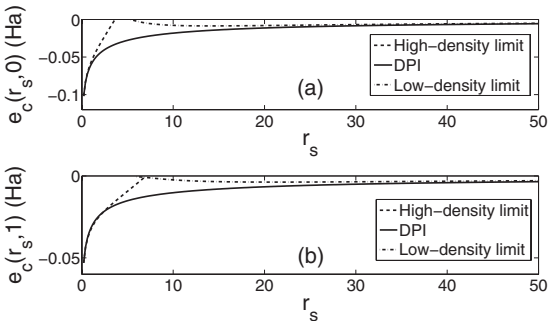

FIG. 1. $e_c(r_s,\zeta=0,1)$ vs r_s using the high-density expansion of Eq. (5) truncated at $n=1$, the low-density expansion of Eq. (6) truncated at $n=2$, and the DPI model.

The leading coefficients in expressions (4)–(6) are listed in Tables I and II. $c_s(\zeta)$ and $c_x(\zeta)$ have simple analytical expressions. The DPI high-density coefficients starred in Table I are exact. Note that these coefficients are all smaller in magnitude (by a factor between 0.34 and 0.68) for $\zeta=1$ than for $\zeta=0$, as expected. Although $a_0(\zeta)$ and $b_0(\zeta)$ are known analytically [Eq. (32) of Ref. 26 or Eqs. (4) and (20) of Ref. 25], they are represented in Table II only by accurate fits since the explicit expressions are rather complicated. The integral expression for $a_1(\zeta)$ (for which RPA is exact) is given in Appendix A, integrated there numerically, and represented in Table II by an accurate fit, too. The performance of these fits is illustrated in Figs. 2(a)–2(c). Figure 2(d) shows our estimate of the coefficient $b_1(\zeta)$ which is not represented in Table II; see Sec. III.

The coefficients $f_{0,1}$ of Eq. (6) given in Table I are evaluated in the simple point charge plus continuum (PC) model of Refs. 30 and 41, and are close to accurately calculated Wigner-crystal values.[42] There is of course no reason to believe that the low-density coefficients f_0, f_1, and f_2 are exactly the same for the uniform fluid as for the Wigner-crystal phase. In the PC model, the pure harmonicity of the electrostatic potential energy of the electron interacting with the uniform sphere of positive charge leads to zero f_2. (The Wigner-crystal value[42] $f_2\neq 0$ arises from anharmonicity.)

The text is organized as follows. Section II provides our interpolation formula between the expansions (5) and (6). The only ingredient that is not known exactly, the coefficient $b_1(\zeta)$ in Eq. (5), is estimated in Sec. III. In Sec. IV, we compare the correlation energies predicted by this simple interpolation to numerical QMC results. Our conclusions are summarized in Sec. V.

II. DENSITY-PARAMETER INTERPOLATION

Apparently, the high-density ($r_s\to 0$) expansion (5) does not have an infinite radius of convergence in r_s. According to Ref. 28, it is an asymptotic expansion with zero radius of convergence. Moreover, its higher-order coefficients (other than the ones listed in Tables I and II) are not fully known. While the situation at medium densities ($r_s\approx 5$) is only accessible by approximate numerical methods (such as QMC calculations), the extreme opposite low-density limit ($r_s\to\infty$) is mathematically simple again, see Eq. (6).

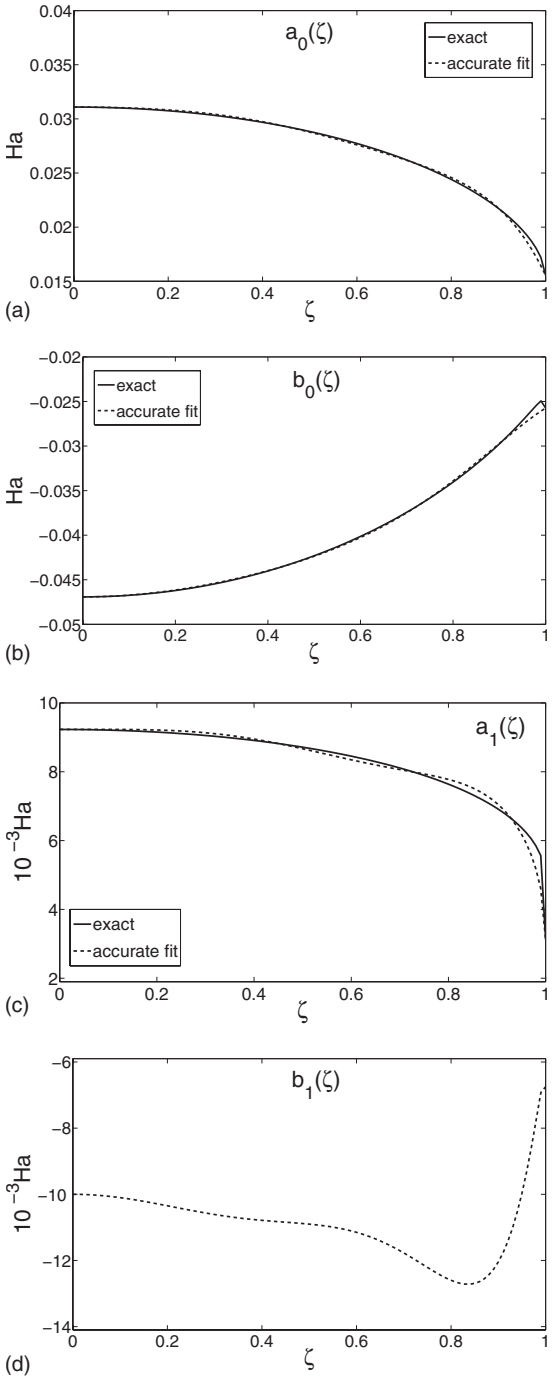

FIG. 2. The ζ dependence of $a_0(\zeta)$, $b_0(\zeta)$, $a_1(\zeta)$, and $b_1(\zeta)$ coefficients. The solid lines in (a), (b), and (c) represent the exact dependence of $a_0(\zeta)$, $b_0(\zeta)$, and $a_1(\zeta)$ while the dashed lines represent the corresponding accurate fits. The exact expressions for $a_0(\zeta)$, $b_0(\zeta)$, and $a_1(\zeta)$ are given by Eq. (32) of Ref. 26 and Eq. (20) of Ref. 25, and in Appendix A, respectively. $b_1(\zeta)$ is given by Eq. (B10) and shown in (d).

To avoid difficulties with the divergent truncated high-density asymptotic expansion (5), we suggest to use only its two leading terms ($n=0,1$) and extrapolate them directly to the leading terms ($n=0,1,2$) of the low-density limit [Eq. (6)],

$$e_c^{\mathrm{DPI}}(r_s,\zeta)=\frac{[a_0(\zeta)+a_1(\zeta)r_s]\ln\frac{r_s}{1+r_s}+b_0(\zeta)+2a_0(\zeta)[1-(1+r_s)^{-1/2}]+b_1(\zeta)\frac{r_s}{1+r_s}}{1+D[1-(1+r_s^2)^{-1/4}]+E[(1+r_s^2)^{1/4}-(1+r_s^2)^{-1/2}]+F[(1+r_s^2)^{1/2}-(1+r_s^2)^{-1/2}]}. \tag{7}$$

Here,

$$F=\frac{b_0(\zeta)-a_1(\zeta)+2a_0(\zeta)+b_1(\zeta)}{f_0-c_x(\zeta)}, \tag{8}$$

$$E=\frac{-f_1}{f_0-c_x(\zeta)}F-\frac{2a_0(\zeta)}{f_0-c_x(\zeta)}, \tag{9}$$

$$D=\frac{-f_1}{f_0-c_x(\zeta)}E-\frac{f_2-c_s(\zeta)}{f_0-c_x(\zeta)}F+\frac{\frac{1}{2}a_1(\zeta)-a_0(\zeta)-b_1(\zeta)}{f_0-c_x(\zeta)}-1. \tag{10}$$

This DPI between the high- and low-density limits $r_s\to 0$ and $r_s\to\infty$ is a smooth analytical function of r_s and ζ. The numerator of Eq. (7) recovers the high-density analytic expansion of Eq. (5) with the correct leading coefficients up to order r_s as $r_s\to 0$ while it tends to the r_s-independent value $b_0(\zeta)-a_1(\zeta)+2a_0(\zeta)+b_1(\zeta)$ as $r_s\to\infty$. In order to recover the $r_s^{-1/2}$ expansion of Eq. (6) in the low-density limit with the correct leading coefficients up to order r_s^{-2}, and to guarantee that the constraints for the high-density limit fulfilled by the numerator are not violated, the denominator is chosen to be a linear combination of $(1+r_s^2)^{m/4}$, with $m=0,\pm 1,\pm 2$. Therefore, unlike previously used formulas, such as Eq. (10) in Ref. 20, Eq. (7) has the right analytic expansions in the two asymptotic limits with the correct coefficients of the leading terms in each of them.

Provided that the exact coefficient $b_1(\zeta)$ is available, Eq. (7) uses only exact information on the extreme high- and low-density limits but no (numerical) information at finite values of r_s. Currently, the exact function $b_1(\zeta)$ has not been evaluated yet, except for the value $b_1(0)=-0.010$.[28] Therefore, we estimate the function $b_1(\zeta)$ in Sec. III.

Figure 1 shows the correlation energy of the unpolarized and fully polarized uniform electron gas. Using the exact information $b_1(0)=-0.010$, the DPI matches the high-density limit expansion for small r_s and is regulated smoothly to the low-density limit expansion for large r_s. For the unpolarized case, no information other than the two limits is used. The exact information $b_1(0)=-0.010$ also enables us to test the DPI model, Eq. (7). Fitting the function $e_c^{\mathrm{DPI}}(r_s,0)$, with $b_1(0)$ as the fitting parameter, to the numerical QMC data of Ref. 10 yields the value $b_1^{\mathrm{fit}}(0)=-0.00757564$, close to the exact one and thus corroborating our DPI model.

III. ESTIMATED COEFFICIENT $b_1(\zeta)$

To estimate the full ζ dependence of $b_1(\zeta)$, we can employ our realistic functional form [Eq. (7)] for a prediction. First we choose the unknown value $b_1(\zeta=1)$ such that the ferromagnetic phase transition of the uniform electron gas occurs at $r_s=75$, as predicted in Ref. 10. This is the only place where numerical information concerning finite values of r_s enters our present DPI model. [In the future, $b_1(1)$ might be evaluated rigorously from perturbation theory.] Furthermore, we choose $b_1(\zeta)$ such that $e_{\mathrm{tot}}^{\mathrm{DPI}}(r_s=75,\zeta)$ becomes strictly independent of ζ. This is a reasonable constraint since it places the divergence of the spin susceptibility at $r_s=75$, somewhat as in the construction of PW92. It is however a simplification of the QMC data of Refs. 13 and 15, which find a continuous magnetic transition with increasing partial spin polarization over the range[15] $50<r_s<100$. With one more parameter, we could fit this more complex behavior.

To this end, note that the explicit expression for $e_{\mathrm{tot}}^{\mathrm{DPI}}(r_s,\zeta)$ is easily solved for $b_1(\zeta)$ since Eq. (7) has the form

$$e_c^{\mathrm{DPI}}(r_s,\zeta)=\frac{I_0(r_s,\zeta)+I_1(r_s)b_1(\zeta)}{J_0(r_s,\zeta)+J_1(r_s,\zeta)b_1(\zeta)} \tag{11}$$

with functions I_0, I_1, J_0, and J_1 that are completely specified by the coefficients in Tables I and II. The detailed expression for $b_1(\zeta)$ is given in Appendix B. It is not strictly monotonic but otherwise reasonably smooth. Figure 2(d) shows $b_1(\zeta)$ constructed with the accurate fits from Table I for $a_0(\zeta)$, $a_1(\zeta)$, and $b_0(\zeta)$.

IV. COMPARISON WITH MONTE CARLO ENERGIES

The DPI correlation energies for $\zeta=0$ and $\zeta=1$ are plotted in Fig. 3(a). Our results are in good agreement with the QMC data of Ref. 10 and comparable to the ones of Ref. 20, from which they differ by less than 0.5 mHa.

In terms of the function,

$$\Delta e_{\mathrm{tot}}(r_s,\zeta)=e_{\mathrm{tot}}(r_s,\zeta)-e_{\mathrm{tot}}(r_s,0), \tag{12}$$

the total-energy difference between the fully polarized ($\zeta=1$) and the unpolarized ($\zeta=0$) phases is given by the function $\Delta e_{\mathrm{tot}}(r_s,1)$, which is plotted versus r_s in Fig. 3(c). This difference is positive for $r_s<75$, indicating that the unpolarized phase with $\zeta=0$ is stable in this case. For $r_s>75$, in contrast, the uniform electron gas is predicted to become ferromagnetic since now the polarized phase with $\zeta=1$ has lower energy than the unpolarized one. To make this phase transition more evident, the behavior around $r_s=75$ is shown in Fig. 3(d) on an expanded scale. $\Delta e_{\mathrm{tot}}^{\mathrm{DPI}}(r_s,1)$ is in good agreement with the corresponding QMC data of Refs. 10 and 15, for the full range of r_s values. This is quite remarkable since we are using no more information on finite r_s values than the value $r_s=75$ of the phase transition itself. By construction, $\Delta e_{\mathrm{tot}}^{\mathrm{DPI}}(r_s,1)$ stays close to (and asymptotically ap-

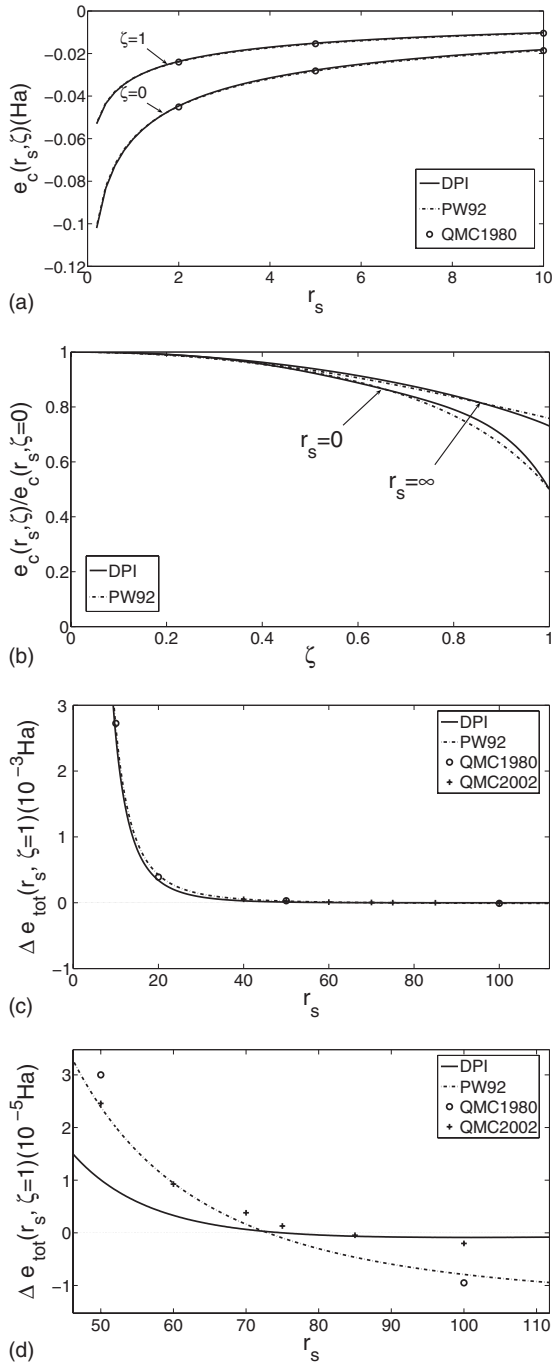

FIG. 3. (a) The DPI correlation energy of the 3D uniform electron gas for the fully spin-polarized ($\zeta=1$) and the unpolarized ($\zeta=0$) phases. (b) $e_c(r_s,\zeta)/e_c(r_s,0)$ vs ζ for $r_s=0$ and $r_s=\infty$. (c) The total-energy difference between the fully spin-polarized ($\zeta=1$) and the unpolarized ($\zeta=0$) phases vs r_s. (d) Zooms around $r_s=75$. QMC1980: Ref. 10. QMC2002: Ref. 15. PW92: Ref. 20.

proaches) the value zero as $r_s\to\infty$ while the corresponding function $\Delta e_{\rm tot}^{\rm PW92}(r_s,1)$ from Ref. 20 does not have the correct low-density ($r_s\to\infty$) behavior (nor do the PZ and VWN forms). It appears from Fig. 3(d) that the QMC of Ref. 10 put the energy of the fully spin-polarized phase too low compared to that of the fully unpolarized phase for $r_s>75$, as corrected in the QMC of Ref. 15. This may have biased all

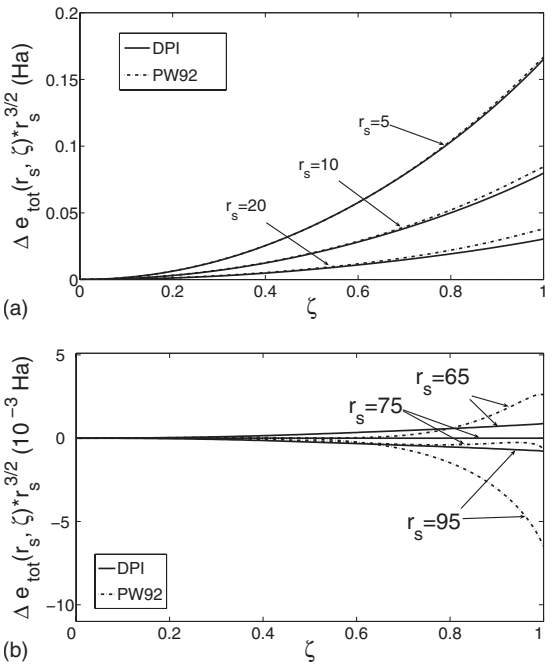

FIG. 4. Total-energy difference times $r_s^{3/2}$ versus spin polarization for $r_s=5$, 10, and 20 in (a) and 65, 75, and 95 in (b), respectively.

the standard parametrizations that relied on Ref. 10, producing values of $f_2(1)$ in Table I that are much too negative.

As a function of ζ, $\Delta e_{\rm tot}^{\rm DPI}(r_s,\zeta)$ is compared in Fig. 4 to $\Delta e_{\rm tot}^{\rm PW92}(r_s,\zeta)$ for selected values of r_s. For small $r_s\leq 20$ [Fig. 4(a)], there is no big difference between the two models. For large $r_s\geq 65$, in contrast [Fig. 4(b)], where DPI still predicts a monotonic ζ dependence, the corresponding curves using Ref. 20 become somewhat irregular.

For $|\zeta|\ll 1$, let $B(r_s,\zeta)\equiv\frac{\zeta}{\chi(r_s)}$ be the magnetic field that holds a given weak "magnetization" ζ. The work $\Delta e_{\rm tot}(r_s,\zeta)$ required to build up this magnetization is $\int_0^\zeta B(r_s,\zeta')d\zeta'$ $\equiv\frac{1}{2}\frac{\zeta^2}{\chi(r_s)}$. Consequently, the r_s-dependent spin susceptibility $\chi(r_s)$ is given by

$$\frac{1}{\chi(r_s)}=\frac{d^2}{d\zeta^2}e_{\rm tot}(r_s,\zeta)|_{\zeta=0}. \tag{13}$$

For noninteracting electrons, with $e_{\rm tot}(r_s,\zeta)=t_s(r_s,\zeta)$, this quantity would be $\chi_0(r_s)=3(\frac{4}{9\pi})^{2/3}r_s^2$. As a function of r_s, the spin susceptibility *enhancement*, $\chi(r_s)/\chi_0(r_s)$, due to exchange and correlation is plotted in Fig. 5. Indicating the phase transition, it has a pole at $r_s=75$ where expression (13) is zero by design.

V. SUMMARY

Extending the early work of Wigner,[2] we have constructed the correlation energy per electron of the uniform electron gas as a pure DPI between exact or nearly exact high- and low-density asymptotes. The high-density information has been found entirely from many-body calculations for the spin-unpolarized case (and could be so found more generally). The low-density information comes from a simple, in-

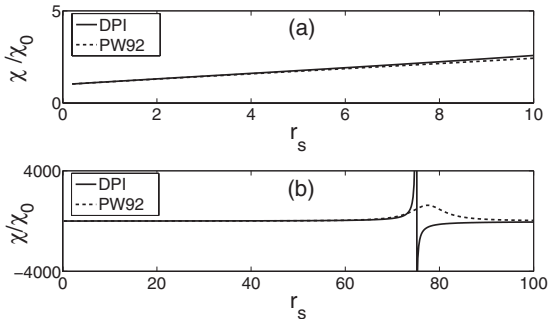

FIG. 5. The spin susceptibility enhancement vs r_s.

tuitive, and accurate model for the total energy, one that is properly independent of relative spin polarization. Our model $e_c^{\mathrm{DPI}}(r_s,\zeta)$, Eq. (7), is accurate for the full ranges of its variables r_s and ζ, comparable to the model $e_c^{\mathrm{PW92}}(r_s,\zeta)$ of Ref. 20. In contrast to the latter, however, the DPI model uses, at least, in principle, (exact) information on the unknown true correlation energy $e_c(r_s,\zeta)$ exclusively from the extreme limits of high ($r_s\to 0$) and low densities ($r_s\to\infty$). Furthermore, unlike VWN and PW92, the DPI model has the correct analytic structure to all orders in both limits. Provided that the coefficient $b_1(\zeta)$ from the high-density ($r_s\to 0$) expansion is known, no numerical QMC data for $e_c(r_s,\zeta)$ at finite values of r_s are required.

Currently, however, $b_1(\zeta)$ is known only for $\zeta=0$. Therefore, we make a compromise and use the single information from the QMC study of Ref. 10 that the ferromagnetic phase transition occurs at $r_s=75$. Forcing in addition that $e_{\mathrm{tot}}^{\mathrm{DPI}}(r_s,\zeta)$ is independent of ζ at $r_s=75$, we predict a reasonably smooth ζ dependence of $b_1(\zeta)$.

The correlation energies predicted by our DPI model for both the unpolarized ($\zeta=0$) and the fully polarized ($\zeta=1$) cases are in excellent agreement with QMC energies. In the extreme limits $r_s\ll 1$ or $r_s\gg 50$, where the high- and low-density asymptotes are, respectively, accurate, the DPI model should be more trustworthy than previous QMC results or parametrizations thereof. In particular, Fig. 3(d) shows (in agreement with later QMC calculations[15]) that the early QMC (Ref. 10) calculation and the standard parametrizations thereof put the energy of the fully polarized system too low relative to that of the unpolarized system at $r_s>75$.

Finally, we point out that it is of great interest to evaluate the exact expression for $b_1(\zeta)$ from perturbation theory. Then, the DPI model of Eq. (7) could be tested for the partly or fully spin-polarized cases, without relying on any numerical QMC data. We would expect therefrom an accuracy sufficient for most density-functional applications, as it is from the widely used parametrizations, although perhaps not sufficient to describe the delicate magnetic phase transition of the low-density uniform phase. At that point, there might be some advantage to finding more accurate fluid-phase values for f_0, f_1, and f_2 from the method of strictly correlated electrons.[43–45]

The widely used PZ, VWN, and PW92 parametrizations of the uniform-gas correlation energy are highly fitted to QMC data, and do not constrain either the low-density expansion coefficients or the high-density ones a_1 and b_1 (although our Table I shows that PW92 extracted reasonable estimates of a_1 and b_1 from QMC data). It is gratifying that the method of constraint satisfaction used to construct many standard density functionals[16,17,46] can also be used to construct their uniform-gas input.

ACKNOWLEDGMENT

This work was supported in part by the National Science Foundation under Grant No. DMR-0854769.

APPENDIX A: EXACT COEFFICIENT $a_1(\zeta)$

For $\zeta=0$, $a_1(\zeta)$ is the sum of Eqs. (16) and (22) in Ref. 27. From Eqs. (10) and (19) there, its ζ dependence can be obtained by spin scaling of the functions $Q_q(u)$, given there by Eq. (11), and $Q_{r_s}^{10}(q,iqu)$, given by Eq. (A3) in Ref. 29. The result is

$$a_1(\zeta)=-\frac{3\alpha}{4\pi^5}\int_{-\infty}^{\infty}du \times[4R(u,\zeta)^2R_1(u,\zeta)-\pi R(u,\zeta)R^{(1)}(iu,\zeta)]. \tag{A1}$$

Here, $\alpha=(\frac{4}{9\pi})^{1/3}$ and

$$R(u,\zeta)=\frac{1}{2}\left[\frac{R(x_1u)}{x_1}+\frac{R(x_2u)}{x_2}\right],$$

$$R_1(u,\zeta)=\frac{1}{2}[x_1R_1(x_1u)+x_2R_1(x_2u)],$$

$$R^{(1)}(iu,\zeta)=\frac{1}{2}[R^{(1)}(ix_1u)+R^{(1)}(ix_2u)]. \tag{A2}$$

In the above expressions, $x_1=(1-\zeta)^{-1/3}$, $x_2=(1+\zeta)^{-1/3}$, and

$$R(u)=1-u\arctan(1/u),$$

$$R_1(u)=-\frac{\pi}{3(1+u^2)^2},$$

$$R^{(1)}(iu)=\frac{4}{1+u^2}[(1+3u^2)-u(2+3u^2)\arctan(u)]. \tag{A3}$$

$R(u)$ and $R_1(u)$ are given by Eqs. (13) and (14) in Ref. 27. $R^{(1)}(iu)$ is given by Eq. (B3) in Ref. 20. Upon numerical integration in Eq. (A1), we find $a_1(0)=9.2292\times10^{-3}$ and $a_1(1)=3.125\times10^{-3}$ [cf. Fig. 2(c)], in agreement with Ref. 20; see Appendix B there.

APPENDIX B: EXPRESSION FOR THE CONSTRUCTED $b_1(\zeta)$

The functions I_0, I_1, J_0, and J_1 of Eq. (11) in Sec. III can be written as

$$I_0 = [a_0(\zeta) + a_1(\zeta) r_s] \ln \frac{r_s}{1 + r_s} + b_0(\zeta) + 2a_0(\zeta)[1 - (1 + r_s)^{-1/2}], \tag{B1}$$

$$I_1 = \frac{r_s}{1 + r_s}, \tag{B2}$$

$$J_n = [1 + (-1)^n]/2 + D_n[1 - (1 + r_s^2)^{-1/4}] + E_n[(1 + r_s^2)^{1/4} - (1 + r_s^2)^{-1/2}] + F_n[(1 + r_s^2)^{1/2} - (1 + r_s^2)^{-1/2}], n = 0, 1. \tag{B3}$$

Here

$$F_0 = \frac{b_0(\zeta) - a_1(\zeta) + 2a_0(\zeta)}{f_0 - c_x(\zeta)}, \tag{B4}$$

$$E_0 = \frac{-f_1}{f_0 - c_x(\zeta)} F_0 - \frac{2a_0(\zeta)}{f_0 - c_x(\zeta)}, \tag{B5}$$

$$D_0 = \frac{-f_1}{f_0 - c_x(\zeta)} E_0 - \frac{f_2 - c_s(\zeta)}{f_0 - c_x(\zeta)} F_0 + \frac{\frac{1}{2} a_1(\zeta) - a_0(\zeta)}{f_0 - c_x(\zeta)} - 1. \tag{B6}$$

$$F_1 = 1/[f_0 - c_x(\zeta)], \tag{B7}$$

$$E_1 = -f_1 F_1^2, \tag{B8}$$

$$D_1 = f_1^2 F_1^3 - [f_2 - c_s(\zeta)] F_1^2 - F_1. \tag{B9}$$

By the construction for $b_1(\zeta)$ in Sec. III, $e_{\rm tot}^{\rm DPI}(r_s^t, \zeta) = e_{\rm tot}^{\rm DPI}(r_s^t, \zeta = 0) = -0.00995977$ Ha at $r_s^t = 75$. Therefore, $b_1(\zeta)$ can be expressed as follows:

$$b_1(\zeta) = \frac{I_0(r_s^t, \zeta) - e_c^{\rm DPI}(r_s^t, \zeta) J_0(r_s^t, \zeta)}{e_c^{\rm DPI}(r_s^t, \zeta) J_1(r_s^t, \zeta) - I_1(r_s^t)} \tag{B10}$$

with

$$e_c^{\rm DPI}(r_s^t, \zeta) = e_{\rm tot}^{\rm DPI}(r_s^t, \zeta = 0) - \frac{c_s(\zeta)}{(r_s^t)^2} - \frac{c_x(\zeta)}{r_s^t}. \tag{B11}$$

[1] G. F. Giuliani and G. Vignale, *Quantum Theory of the Electron Fluid* (Cambridge University Press, Cambridge, 2005).
[2] E. P. Wigner, Phys. Rev. **46**, 1002 (1934); Trans. Faraday Soc. **34**, 678 (1938).
[3] W. Macke, Z. Naturforsch. **5A**, 192 (1950).
[4] D. Bohm and D. Pines, Phys. Rev. **92**, 609 (1953).
[5] M. Gell-Mann and K. A. Brueckner, Phys. Rev. **106**, 364 (1957).
[6] K. S. Singwi, A. Sjoelander, M. P. Tosi, and R. H. Land, Phys. Rev. B **1**, 1044 (1970).
[7] D. L. Freeman, Phys. Rev. B **15**, 5512 (1977).
[8] L. A. Constantin, J. M. Pitarke, J. F. Dobson, A. Garcia-Lekue, and J. P. Perdew, Phys. Rev. Lett. **100**, 036401 (2008).
[9] A. Grüneis, M. Marsman, J. Harl, L. Schimka, and G. Kresse, J. Chem. Phys. **131**, 154115 (2009).
[10] D. M. Ceperley and B. J. Alder, Phys. Rev. Lett. **45**, 566 (1980).
[11] B. Tanatar and D. M. Ceperley, Phys. Rev. B **39**, 5005 (1989).
[12] G. Ortiz and P. Ballone, Phys. Rev. B **56**, 9970 (1997).
[13] G. Ortiz, M. Harris, and P. Ballone, Phys. Rev. Lett. **82**, 5317 (1999).
[14] D. Varsano, S. Moroni, and G. Senatore, Europhys. Lett. **53**, 348 (2001).
[15] F. H. Zong, C. Lin, and D. M. Ceperley, Phys. Rev. E **66**, 036703 (2002).
[16] W. Kohn and L. J. Sham, Phys. Rev. **140**, A1133 (1965).
[17] J. P. Perdew and S. Kurth, in *A Primer in Density Functional Theory*, Lecture Notes in Physics Vol. 620, edited by C. Fiolhais, F. Nogueira, and M. Marques (Springer, New York, 2003).
[18] J. P. Perdew and A. Zunger, Phys. Rev. B **23**, 5048 (1981).
[19] S. H. Vosko, L. Wilk, and M. Nusair, Can. J. Phys. **58**, 1200 (1980).
[20] J. P. Perdew and Y. Wang, Phys. Rev. B **45**, 13244 (1992).
[21] J. P. Perdew, J. Tao, and S. Kuemmel, in *Electron Correlation Methodology*, ACS Symposium Series Vol. **958**, edited by A. K. Wilson and K. A. Peterson (American Chemical Society, Washington, DC, 2007).
[22] M. Filatov and W. Thiel, Int. J. Quantum Chem. **62**, 603 (1997).
[23] E. Proynov and J. Kong, Phys. Rev. A **79**, 014103 (2009).
[24] L. Onsager, L. Mittag, and M. J. Stephen, Ann. Phys. (Leipzig) **473**, 71 (1966).
[25] G. G. Hoffman, Phys. Rev. B **45**, 8730 (1992).
[26] Y. Wang and J. P. Perdew, Phys. Rev. B **43**, 8911 (1991).
[27] W. J. Carr and A. A. Maradudin, Phys. Rev. **133**, A371 (1964).
[28] T. Endo, M. Horiuchi, Y. Takada, and H. Yasuhara, Phys. Rev. B **59**, 7367 (1999).
[29] D. F. DuBois, Ann. Phys. (N. Y.) **7**, 174 (1959).
[30] M. Seidl, J. P. Perdew, and S. Kurth, Phys. Rev. A **62**, 012502 (2000); **72**, 029904(E) (2005).
[31] M. Seidl, J. P. Perdew, and S. Kurth, Phys. Rev. Lett. **84**, 5070 (2000).
[32] P. Mori-Sanchez, A. J. Cohen, and W. Yang, J. Chem. Phys. **124**, 091102 (2006).
[33] A. J. Cohen, P. Mori-Sanchez, and W. Yang, J. Chem. Phys. **126**, 191109 (2007).
[34] Z. Yan, J. P. Perdew, S. Kurth, C. Fiolhais, and L. Almeida, Phys. Rev. B **61**, 2595 (2000); **64**, 049904 (2001).
[35] P. H. Acioli and D. M. Ceperley, Phys. Rev. B **54**, 17199 (1996).
[36] P. Ballone, C. J. Umrigar, and P. Delaly, Phys. Rev. B **45**, 6293 (1992).
[37] B. Wood, N. D. M. Hine, W. M. C. Foulkes, and P. Garcia-Gonzalez, Phys. Rev. B **76**, 035403 (2007).
[38] P. Ziesche, J. Tao, M. Seidl, and J. P. Perdew, Int. J. Quantum Chem. **77**, 819 (2000).
[39] P. Ziesche and J. Cioslowki, Physica A **356**, 598 (2005).
[40] V. C. Aguilera-Navarro, G. A. Baker, Jr., and M. de Llano, Phys.

Rev. B **32**, 4502 (1985).
[41] M. Seidl, J. P. Perdew, and M. Levy, Phys. Rev. A **59**, 51 (1999).
[42] W. J. Carr, R. A. Coldwell-Horsfall, and A. E. Fein, Phys. Rev. **124**, 747 (1961).
[43] M. Seidl, P. Gori-Giorgi, and A. Savin, Phys. Rev. A **75**, 042511 (2007).
[44] P. Gori-Giorgi, G. Vignale, and M. Seidl, J. Chem. Theory Comput. **5**, 743 (2009).
[45] P. Gori-Giorgi, M. Seidl, and G. Vignale, Phys. Rev. Lett. **103**, 166402 (2009).
[46] J. P. Perdew, A. Ruzsinszky, G. I. Csonka, L. A. Constantin, and J. Sun, Phys. Rev. Lett. **103**, 026403 (2009).